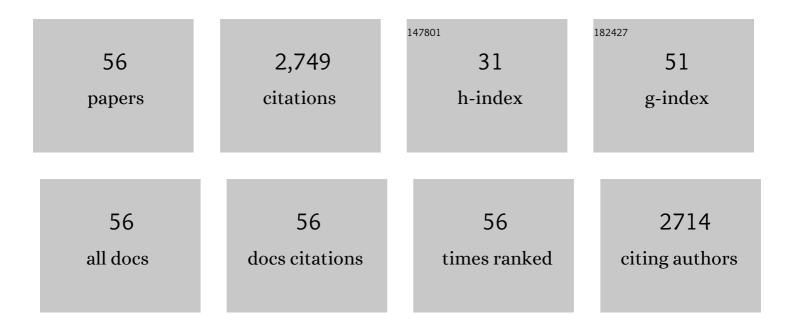


## List of Publications by Year in descending order

Source: https://exaly.com/author-pdf/2468180/publications.pdf Version: 2024-02-01



CHAOLI

#	Article	IF	CITATIONS
1	Mesoporous nanostructured Co <sub>3</sub> O <sub>4</sub> derived from MOF template: a high-performance anode material for lithium-ion batteries. Journal of Materials Chemistry A, 2015, 3, 5585-5591.	10.3	255
2	High Anodic Performance of Co 1,3,5-Benzenetricarboxylate Coordination Polymers for Li-Ion Battery. ACS Applied Materials & Interfaces, 2016, 8, 15352-15360.	8.0	181
3	Pristine MOF and COF materials for advanced batteries. Energy Storage Materials, 2020, 31, 115-134.	18.0	149
4	Ultrathin Manganese-Based Metal–Organic Framework Nanosheets: Low-Cost and Energy-Dense Lithium Storage Anodes with the Coexistence of Metal and Ligand Redox Activities. ACS Applied Materials & Interfaces, 2017, 9, 29829-29838.	8.0	131
5	Cobalt-based metal organic framework with superior lithium anodic performance. Journal of Solid State Chemistry, 2016, 242, 71-76.	2.9	130
6	The organic-moiety-dominated Li <sup>+</sup> intercalation/deintercalation mechanism of a cobalt-based metal–organic framework. Journal of Materials Chemistry A, 2016, 4, 16245-16251.	10.3	116
7	A thermally activated manganese 1,4-benzenedicarboxylate metal organic framework with high anodic capability for Li-ion batteries. New Journal of Chemistry, 2016, 40, 9746-9752.	2.8	104
8	Hierarchical CuO octahedra inherited from copper metal–organic frameworks: high-rate and high-capacity lithium-ion storage materials stimulated by pseudocapacitance. Journal of Materials Chemistry A, 2017, 5, 12828-12837.	10.3	80
9	Facile synthesis of the Basolite F300-like nanoscale Fe-BTC framework and its lithium storage properties. RSC Advances, 2016, 6, 114483-114490.	3.6	79
10	Ultrathin Cobaltâ€Based Metal–Organic Framework Nanosheets with Both Metal and Ligand Redox Activities for Superior Lithium Storage. Chemistry - A European Journal, 2017, 23, 15984-15990.	3.3	77
11	Unraveling the Critical Role of Ti Substitution in P <sub>2</sub> -Na <sub><i>x</i></sub> Li <sub><i>y</i></sub> Mn <sub>1–<i>y</i></sub> O <sub>2</sub> Cathodes for Highly Reversible Oxygen Redox Chemistry. Chemistry of Materials, 2020, 32, 1054-1063.	6.7	74
12	Cobalt(II) dicarboxylate-based metal-organic framework for long-cycling and high-rate potassium-ion battery anode. Electrochimica Acta, 2017, 253, 439-444.	5.2	67
13	Bimetallic coordination polymer as a promising anode material for lithium-ion batteries. Chemical Communications, 2016, 52, 2035-2038.	4.1	65
14	Green and Rational Design of 3D Layer-by-Layer MnO <i><sub>x</sub></i> Hierarchically Mesoporous Microcuboids from MOF Templates for High-Rate and Long-Life Li-Ion Batteries. ACS Applied Materials & Interfaces, 2018, 10, 14684-14697.	8.0	55
15	Coexistence of (O <sub>2</sub> ) <sup><i>n</i>â^'</sup> and Trapped Molecular O <sub>2</sub> as the Oxidized Species in P2-Type Sodium 3d Layered Oxide and Stable Interface Enabled by Highly Fluorinated Electrolyte. Journal of the American Chemical Society, 2021, 143, 18652-18664.	13.7	55
16	Remarkable improvement in the lithium storage property of Co2(OH)2BDC MOF by covalent stitching to graphene and the redox chemistry boosted by delocalized electron spins. Chemical Engineering Journal, 2017, 326, 1000-1008.	12.7	53
17	Carbon-coated Li3V2(PO4)3 derived from metal-organic framework as cathode for lithium-ion batteries with high stability. Electrochimica Acta, 2018, 271, 608-616.	5.2	52
18	High Ethylene Selectivity in Methanolâ€ŧoâ€Olefin (MTO) Reaction over MORâ€Zeolite Nanosheets. Angewandte Chemie - International Edition, 2020, 59, 6258-6262.	13.8	46

Chao Li

#	Article	IF	CITATIONS
19	Reversible lithium storage in manganese and cobalt 1,2,4,5-benzenetetracarboxylate metal–organic framework with high capacity. RSC Advances, 2016, 6, 61319-61324.	3.6	45
20	Capacity control of ferric coordination polymers by zinc nitrate for lithium-ion batteries. RSC Advances, 2016, 6, 86126-86130.	3.6	42
21	Exploring the Capacity Limit: A Layered Hexacarboxylate-Based Metal–Organic Framework for Advanced Lithium Storage. Inorganic Chemistry, 2018, 57, 3126-3132.	4.0	41
22	Investigating the Electrochemical Behavior of Cobalt(II) Terephthalate (CoC8H4O4) as the Organic Anode in K-ion Battery. Electrochimica Acta, 2017, 253, 333-338.	5.2	40
23	High-energy nanostructured Na <sub>3</sub> V <sub>2</sub> (PO <sub>4</sub> ) <sub>2</sub> O <sub>1.6</sub> F <sub>1.4</sub> cathodes for sodium-ion batteries and a new insight into their redox chemistry. Journal of Materials Chemistry A. 2018. 6. 8340-8348.	10.3	39
24	Bimetallic zeolite imidazolate framework for enhanced lithium storage boosted by the redox participation of nitrogen atoms. Science China Materials, 2018, 61, 1040-1048.	6.3	39
25	Reversible phase transition enabled by binary Ba and Ti-based surface modification for high voltage LiCoO2 cathode. Journal of Power Sources, 2019, 438, 226954.	7.8	38
26	Restraining Oxygen Loss and Boosting Reversible Oxygen Redox in a P2-Type Oxide Cathode by Trace Anion Substitution. ACS Applied Materials & Interfaces, 2021, 13, 360-369.	8.0	38
27	Anionic redox reactions and structural degradation in a cation-disordered rock-salt Li <sub>1.2</sub> Ti <sub>0.4</sub> Mn <sub>0.4</sub> O <sub>2</sub> cathode material revealed by solid-state NMR and EPR. Journal of Materials Chemistry A, 2020, 8, 16515-16526.	10.3	37
28	The electrochemical Na intercalation/extraction mechanism of ultrathin cobalt(II) terephthalate-based MOF nanosheets revealed by synchrotron X-ray absorption spectroscopy. Energy Storage Materials, 2018, 14, 82-89.	18.0	35
29	Unraveling the Redox Couples of V <sup>III</sup> /V <sup>IV</sup> Mixed-Valent Na <sub>3</sub> V <sub>2</sub> (PO <sub>4</sub> ) <sub>2</sub> O <sub>1.6</sub> F <sub>1.4</sub> Cathode by Parallel-Mode EPR and In Situ/Ex Situ NMR. Journal of Physical Chemistry C, 2018, 122, 27224-27232.	3.1	35
30	Anionic redox reaction in Na-deficient layered oxide cathodes: Role of Sn/Zr substituents and in-depth local structural transformation revealed by solid-state NMR. Energy Storage Materials, 2021, 39, 60-69.	18.0	35
31	One-Pot Synthesis of Co-Based Coordination Polymer Nanowire for Li-Ion Batteries with Great Capacity and Stable Cycling Stability. Nano-Micro Letters, 2018, 10, 19.	27.0	33
32	High Ethylene Selectivity in Methanolâ€toâ€Olefin (MTO) Reaction over MORâ€Zeolite Nanosheets. Angewandte Chemie, 2020, 132, 6317-6321.	2.0	33
33	MOFs and their derivatives as Sn-based anode materials for lithium/sodium ion batteries. Journal of Materials Chemistry A, 2021, 9, 27234-27251.	10.3	33
34	Room-temperature synthesis of a cobalt 2,3,5,6-tetrafluoroterephthalic coordination polymer with enhanced capacity and cycling stability for lithium batteries. New Journal of Chemistry, 2017, 41, 1813-1819.	2.8	31
35	Highly reversible lithium storage in cobalt 2,5-dioxido-1,4-benzenedicarboxylate metal-organic frameworks boosted by pseudocapacitance. Journal of Colloid and Interface Science, 2017, 506, 365-372.	9.4	31
36	Deciphering the Origin of High Electrochemical Performance in a Novel Ti-Substituted P2/O3 Biphasic Cathode for Sodium-Ion Batteries. ACS Applied Materials & Interfaces, 2020, 12, 41485-41494.	8.0	31

Chao Li

#	Article	IF	CITATIONS
37	High-capacity cobalt-based coordination polymer nanorods and their redox chemistry triggered by delocalization of electron spins. Energy Storage Materials, 2017, 7, 195-202.	18.0	28
38	Mitigating voltage decay in high-capacity Li1.2Ni0.2Mn0.6O2 cathode material by surface K+ doping. Electrochimica Acta, 2018, 291, 278-286.	5.2	27
39	Mapping the Distribution and the Microstructural Dimensions of Metallic Lithium Deposits in an Anode-Free Battery by In Situ EPR Imaging. Chemistry of Materials, 2021, 33, 8223-8234.	6.7	24
40	Multi-thiol-supported dicarboxylate-based metal–organic framework with excellent performance for lithium-ion battery. Chemical Engineering Journal, 2022, 431, 133234.	12.7	23
41	What Triggers the Voltage Hysteresis Variation beyond the First Cycle in Li-Rich 3d Layered Oxides with Reversible Cation Migration?. Journal of Physical Chemistry Letters, 2021, 12, 8740-8748.	4.6	21
42	Unveiling the benefits of potassium doping on the structural integrity of Li–Mn-rich layered oxides during prolonged cycling by dual-mode EPR spectroscopy. Physical Chemistry Chemical Physics, 2019, 21, 24017-24025.	2.8	19
43	Operando EPR and EPR Imaging Study on a NaCrO <sub>2</sub> Cathode: Electronic Property and Structural Degradation with Cr Dissolution. Journal of Physical Chemistry Letters, 2021, 12, 781-786.	4.6	19
44	Tailoring Anionic Redox Activity in a P2-Type Sodium Layered Oxide Cathode via Cu Substitution. ACS Applied Materials & Interfaces, 2022, 14, 28738-28747.	8.0	18
45	Triggering and Stabilizing Oxygen Redox Chemistry in Layered Li[Na <sub>1/3</sub> Ru <sub>2/3</sub> ]O <sub>2</sub> Enabled by Stable Li–O–Na Configuration. ACS Energy Letters, 2022, 7, 2349-2356.	17.4	18
46	A multifunctional manipulation to stabilize oxygen redox and phase transition in 4.6 V high-voltage LiCoO2 with sXAS and EPR studies. Journal of Power Sources, 2021, 516, 230661.	7.8	17
47	Stable electronic structure related with Mn4+Oâ^'• coupling determines the anomalous nonhysteretic behavior in Na2Mn3O7. Energy Storage Materials, 2022, 48, 290-296.	18.0	16
48	Controlled synthesis of Co <sub>x</sub> Mn <sub>3â^'x</sub> O <sub>4</sub> nanoparticles with a tunable composition and size for high performance lithium-ion batteries. RSC Advances, 2016, 6, 54270-54276.	3.6	14
49	Amorphization and disordering of metal–organic framework materials for rechargeable batteries by thermal treatment. New Journal of Chemistry, 2017, 41, 6415-6419.	2.8	14
50	Reversible High-Voltage N-Redox Chemistry in Metal–Organic Frameworks for High-Rate Anion-Intercalation Batteries. ACS Applied Energy Materials, 2019, 2, 413-419.	5.1	14
51	NMR Evidence for the Multielectron Reaction Mechanism of Na <sub>3</sub> V <sub>2</sub> (PO <sub>4</sub> ) <sub>3</sub> Cathode and the Impact of Polyanion Site Substitution. Journal of Physical Chemistry C, 2021, 125, 15200-15209.	3.1	11
52	Coincident formation of trapped molecular O2 in oxygen-redox-active archetypical Li 3d oxide cathodes unveiled by EPR spectroscopy. Energy Storage Materials, 2022, 50, 55-62.	18.0	11
53	A green ligand-based copper–organic framework: a high-capacity lithium storage material and insight into its abnormal capacity-increase behavior. New Journal of Chemistry, 2020, 44, 17899-17905.	2.8	10
54	Retarding Phase Transformation During Cycling in a Lithium―and Manganeseâ€Rich Cathode Material by Optimizing Synthesis Conditions. ChemElectroChem, 2019, 6, 1385-1392.	3.4	8

#	Article	IF	CITATIONS
55	Reduction of the 13C cross-polarization experimental time for pharmaceutical samples with long T1 by ball milling in solid-state NMR. Solid State Nuclear Magnetic Resonance, 2018, 94, 20-25.	2.3	6
56	Na <sub>3</sub> V <sub>2</sub> (PO <sub>4</sub> ) <sub>3</sub> Revisited: A High-Resolution Solid-State NMR Study. Journal of Physical Chemistry C, 2021, 125, 24060-24066.	3.1	6